Fizika Nizkikh Temperatur, 2007, v. 33, Nos. 2/3, p. 256–262

Vertical spin transport in semiconductor heterostructures

P. Sankowski[1], P. Kacman[1], J.A. Majewski[2], and T. Dietl[1,2,3]

[1] *Institute of Physics, Polish Academy of Sciences, 32/46 al. Lotnikow, Warszawa 02668, Poland*

[2] *Institute of Theoretical Physics, Warsaw University, 69 ul. Hoza, Warszawa 00681, Poland*
E-mail: jacek.majewski@fuw.edu.pl

[3] *ERATO Semiconductor Spintronics Project*

Received September 22, 2006

The Landauer–Büttiker formalism combined with the tight-binding transfer matrix method is employed to model vertical coherent spin transport within magnetization modulated semiconductor heterostructures based on GaAs. This formalism provides excellent physical description of recent experiments concerning the high tunneling magnetoresistance (TMR) in (Ga,Mn)As-based trilayers and highly polarized spin injection in *p*-(Ga,Mn)As/*n*-GaAs Zener diode. For both the TMR and the Zener spin current polarization, the calculated values compare well with those observed in the experiments and the formalism reproduces the strong decrease of the observed effects with external bias. We ascribe this decrease to the band structure effects. The role played in the spin dependent tunneling by carrier concentration and magnetic ion content is also studied.

PACS: 75.50.Pp Magnetic semiconductors;
72.25.Hg Electrical injection of spin polarized carriers;
73.40.Gk Tunneling.

Keywords: ferromagnetic semiconductors, spin transport, tunneling magnetoresistance.

1. Introduction

With the recent discovery of ferromagnetic semiconductors [1] compatible with III–V epitaxy [2] the field of spintronics has expanded from all-metal [3,4] and hybrid metal–semiconductor [5] structures to include all-semiconductor ferromagnetic devices [6]. Such devices have revealed intriguing properties, such as control of their Curie temperature with an applied voltage [7]. This is a consequence of the carrier-mediated nature of the ferromagnetism in these materials, which allows manipulation of the magnetic properties through control of the electronic subsystem (i.e., through doping, gating, etc.) [8].

(Ga,Mn)As is believed to be one of the most promising materials for semiconductor spintronics. First of all, it has almost the same lattice constant as GaAs and AlAs, and with the (Ga,Mn)As/III–V heterostructures one can form high-quality all-semiconductor spintronic devices, such as magnetic tunnel junctions. In addition, (Ga,Mn)As, based devices might be easily integrated within other III–V-based devices. Moreover, in recent years the optimization of the conditions of MBE growth and post-growth annealing of (Ga,Mn)As has resulted in a still rapid increase of the Curie temperature in this compound, which now reaches 173 K [9].

Spin-dependent phenomena in modulated magnetic semiconductors attract a lot of interest due to the possible applications in spintronic devices. One of the fundamental prerequisites for construction of functional spintronic devices, such as spin transistors [10], is efficient spin injection from ferromagnetic regions into the paramagnetic ones. On the other hand, the tunneling magnetoresistance (TMR) effect, discovered by Júlliere in a Co/Ge/Fe structure [11], has already found many applications in magnetic field sensors and magnetic random access memories, for example. Both these phenomena have been also recently observed in (Ga,Mn)As-based structures. It has been demonstrated that highly spin-polarized electron current (about 80%) can indeed be obtained from *p*-(Ga,Mn)As/*n*-GaAs Zener diode [12]. Also a high (of about 75%) TMR effect in (Ga,Mn)As/AlAs/(Ga,Mn)As trilayers was presen-

© P. Sankowski, P. Kacman, J.A. Majewski, and T. Dietl, 2007

ted first by Tanaka and Higo [13]. Recent experiments exhibit TMR even as high as 250% [14–16].

The further developement of spintronic devices requires deep understanding of vertical spin transport and a modeling tool that facilitates the design of new devices. Since the ferromagnetic coupling in (Ga,Mn)As is mediated by the holes [1,8], a meaningful theory has to take into account the entire complexity of the valence band, including the spin–orbit interaction. Furthermore, the intermixing of valence bands caused by spin–orbit coupling shortens the spin diffusion length and makes it comparable to the phase coherence length. This renders the models based on the classical spin-diffusion equation, which describe satisfactorily the spin transport phenomena in metallic MTJs, nonapplicable directly to the structures containing layers of hole-controlled diluted ferromagnetic semiconductors.

Recently, we have developed a computational scheme for vertical coherent spin transport. This model combines the two-terminal Landauer–Büttiker formalism with the empirical multi-orbital tight-binding description of the semiconductor band structure. In this way, the quantum character of spin transport over the length scale relevant for the devices in question is taken into account.

Furthermore, the tight-binding approach, in contrast to *kp* models employed so-far [17,18], allows for a proper description of effects crucial for spin transport in heterostructures such as atomic structure of interfaces, effects of Rashba and Dresselhaus terms, as well as tunnel involving **k** states away from the center of the Brillouin zone. Our model has recently been applied to describe selected features of Zener–Esaki diodes [19,20] and TMR devices [20] and has also been as well as it was adopted to examine an intrinsic domain-wall resistance in (Ga,Mn)As [21].

The present paper is organized as follows. In Sec. 2, we present the basics of the formalism employed. In Secs. 3 and 4, we discuss two basic phenomena mentioned above, namely, the injection of spin polarized valence electrons into the conduction band of GaAs realized in the *p*-(Ga,Mn)As/*n*-GaAs Zener diode, and TMR effect in (Ga,Mn)As/GaAs/(Ga,Mn)As structures.

2. Theoretical model

We consider a prototype heterostructure which is uniform and infinite in the x and y directions, has modulated magnetization along the z ([001]) growth direction, and is connected to two semi-infinite bulk contacts denoted by L and R. In all cases considered, we assume that the bias is applied in such a way that spin-polarized carriers are injected from the ferromagnetic left lead. Our goal is to calculate the electric current in the structure and the degree of current spin polarization outside the left lead. The typical length of the structures studied is comparable to the phase coherence length. Therefore, we restrict ourselves to the vertical coherent transport regime that we treat within Landauer–Büttiker formalism, where the current is determined by the transmission probability of the ingoing Bloch state at the left contact into the outgoing Bloch state at the right contact. In the presence of spin–orbit coupling, the spin is not a good quantum number. The only conserved quantities in tunneling are the energy E and, due to the spatial in-plane symmetry of our structures, the in-plane wave vector $\mathbf{k}_{||}$. We use semi-empirical tight-binding formalism to calculate electronic states of the system for given $\mathbf{k}_{||}$ and E and further compute transmission coefficients.

2.1. Tight-binding model

First, we describe the construction of the tight-binding Hamiltonian matrix for «normal» GaAs and AlAs as well as ferromagnetic (Ga,Mn)As layers of the heterostructure. To describe the band structure of the bulk GaAs and bulk AlAs, we use the nearest neighbor (NN) $sp^3d^5s^*$ tight–binding Hamiltonian (resulting in 20 spin-orbitals for each anion or cation), with the spin-orbit coupling included [22]. This model reproduces correctly the effective masses and the band structure of GaAs and AlAs in the whole Brillouin zone. With the tight-binding Hamiltonian introduced above, each double layer (cation + anion) is represented by 40×40 matrix. It should be pointed out that the d orbitals used in our $sp^3d^5s^*$ parametrization are not related to the 3d semi-core states and are of no use for description of Mn ions incorporated into GaAs. The presence of Mn ions in (Ga,Mn)As is taken into account by including the (sp–d)-exchange interactions within the virtual crystal and mean-field approximations. In the spirit of the tight-binding method, the effects of an external interaction are included in the on-site diagonal matrix elements of the tight-binding Hamiltonian. Here, the shifts of on-site energies caused by the (sp–d)-exchange interaction are parameterized in such a way that they reproduce experimentally obtained spin splitting: $N_0\alpha = 0.2$ eV for the conduction band, and $N_0\beta = -1.2$ eV for the valence band [23]. The other parameters of the model for the (Ga,Mn)As material and for the NN interactions between GaAs and (Ga,Mn)As are taken to be the same as for GaAs. This is well motivated because the valence-band structure of (Ga,Mn)As with small fraction of Mn has been shown to be quite similar to that of GaAs [23]. Consequently, the valence band offset between (Ga,Mn)As and GaAs originates only from

the spin splitting of the bands in (Ga,Mn)As. The Fermi energy in the constituent materials is determined by the assumed carrier concentration and is calculated from the density of states obtained for tight-binding Hamiltonian. Our calculations of the Fermi energy for various hole concentrations are consistent with the corresponding results presented in Ref. 8.

Having determined the Hamiltonian of the system, we are now in the position to define the current and current spin polarization in the presence of spin–orbit coupling.

2.2. Current and current spin polarization

For a given energy E and in-plane wave-vector $k_{||}$, the Bloch states in the left L and right R leads (i and j, respectively) are characterized by the wave vector component $k_{\perp}$ perpendicular to the layers and are denoted by $|L, k_{L,\perp,i}\rangle$ and $|R, k_{R,\perp,j}\rangle$, respectively. The indices i and j indicate all possible pairs for 40 bands described by the tight-binding Hamiltonian. The transmission probability $T_{L,k_{L,\perp,i}\to R,k_{R,\perp,j}}$ is a function of the transmission amplitude $t_{L,k_{L,\perp,i}\to R,k_{R,\perp,j}}(E,\mathbf{k}_{||})$ and group velocities in the left and right lead, $v_{L,\perp,i}$ and $v_{R,\perp,j}$:

$$T_{L,k_{L,\perp,i}\to R,k_{R,\perp,j}}(E,\mathbf{k}_{||}) = \left| t_{L,k_{L,\perp,i}\to R,k_{R,\perp,j}}(E,\mathbf{k}_{||})\right|^2 \frac{v_{R,\perp,j}}{v_{L,\perp,i}}. \quad (1)$$

The current flowing in the rightward direction can now be written as [24]

$$j_{L\to R} = \frac{-e}{(2\pi)^3\hbar}\int_{BZ} d^2k_{||}\, dEf_L(E) \times \sum_{\substack{k_{L,\perp,i},k_{R,\perp,j}\\ v_{L,\perp,i},v_{R,\perp,j}>0}} T_{L,k_{L,\perp,i}\to R,k_{R,\perp,j}}(E,\mathbf{k}_{||}), \quad (2)$$

where f_L or respectively f_R are the electron Fermi distributions in the left and right interface and i, j number the corresponding Bloch states. Plugging in the expresion given in Eq. (1) and using the time reversal symmetry:

$$T_{L,k_{L,\perp,i}\to R,k_{R,\perp,j}}(E,\mathbf{k}_{||}) = T_{L,-k_{R,\perp,j}\to R,-k_{L,\perp,i}}(E,\mathbf{k}_{||}), \quad (3)$$

we get

$$j = \frac{-e}{(2\pi)^3\hbar}\int_{BZ} d^2k_{||}\, dE\left[f_L(E) - f_R(E)\right] \times \sum_{\substack{k_{L,\perp,i},k_{R,\perp,j}\\ v_{L,\perp,i},v_{R,\perp,j}>0}} \left| t_{L,k_{L,\perp,i}\to R,k_{R,\perp,j}}(E,\mathbf{k}_{||})\right|^2 \frac{v_{R,\perp,j}}{v_{L,\perp,i}}. \quad (4)$$

To calculate the current one has to determine the transmission probability, and thus the transmission amplitude $t_{L,k_{L,\perp,i}\to k_{R,R,\perp,j}}(E,\mathbf{k}_{||})$ and the group velocities $v_{L,\perp,j}$ of the ingoing and $v_{R,\perp,j}$ of the outgoing states. These can be obtained by solving the Schrödinger equation for the structure with appropriate scattering boundary conditions. In our studies, we follow closely the procedure detailed in Refs. 25 and 26, which we have generalized to the case with spin–orbit coupling.

In the studies of the Zener tunneling diode, we are mostly interested in the degradation of the spin polarization of carriers passing from the source (Ga,Mn)As to a paramagnetic n-GaAs drain. To quantify this degradation, we introduce the spin polarization of the outgoing Bloch state [27] defined as

$$P_{R,k_{R,\perp,i}}(E,\mathbf{k}_{||}) = \langle R,k_{R,\perp,i}|\boldsymbol{\Omega}\cdot\mathbf{s}|R,k_{R,\perp,i}\rangle, \quad (5)$$

where $\boldsymbol{\Omega}$ is the direction of the spontaneous magnetization in the ferromagnetic semiconductor and $\mathbf{s}$ is the spin operator. Then, we can define the total spin polarized current:

$$j_s = \frac{-e}{(2\pi)^3\hbar}\int_{BZ} d^2k_{||}\, dE\,[f_L(E) - f_R(E)] \times \sum_{\substack{k_{L,\perp,i},k_{R,\perp,j}\\ v_{L,\perp,i},v_{R,\perp,j}>0}} T_{L,k_{L,\perp,i}\to R,k_{R,\perp,j}}(E,\mathbf{k}_{||})P_{R,k_{R,\perp,i}}. \quad (6)$$

The spin polarization of the coherently transmitted current is now equal to

$$P_s = \frac{j_s}{j}. \quad (7)$$

This scheme follows closely some ideas introduced recently in studies of the spin depolarization of holes in the (Ga,Mn)As/GaAlAs/p-GaAs structures [27] and will be employed to analyze the spin polarization of current in the Zener tunnel diode.

3. Results and discussion

In this Section we employ the formalism described in the previous Section to the structures studied experimentally. We start the discussion with the Zener tunnel diode and further we discuss TMR structures based on (Ga,Mn)As ferromagnetic semiconductors.

3.1. Zener tunnel diode

A rather high ≈ 80% spin polarization of the tunneling electrons from the valence band of (Ga,Mn)As to the GaAs conduction band has been recently obtained in Zener diodes [12,28]. This opens new perspectives for applications of electron spin injection. However, the experimentally observed degree of current spin polarization exhibits a sharp decrease with the applied bias [12,28]. In the present paper we analyze theoretically the transport in the Zener diode structures as a function of the applied bias employing the developed theoretical scheme involving transfer matrix formalism described in Sec. 2. However, within this formalism, one is not able to consider the whole structure investigated experimentally, because of computational constraints. Therefore, we perform the analysis of the intriguing phenomenon of current drop with applied bias in two steps. First, we model the charge transport in the entire Zener diode (corresponding to the experimental structure) under bias using continuum theory and a commercial simulation tool [19]. This allows self-consistent calculations of semiconductor heterostructures taking into account band-to-band tunneling, recombination, and impact ionization. By these simulations a detailed understanding of the charge distribution and the band lineup in the entire device can be achieved. Next, we consider the most essential part of the device consisting of p-$Ga_{1-x}Mn_xAs/n$-GaAs tunnel junction using the calculated potential profile in the tight-binding Hamiltonian. According to the self-consistent calculations, the scattering region consists of approximately 120 monolayers of $Ga_{1-x}Mn_xAs$ and GaAs, and corresponds roughly to the depletion zone of the diode. In Fig. 1 we show the calculated potential profile in the structures used in experiments [12]. This potential profile has been obtained in self-consistent calculations for external reverse bias of V_0 = 1.8 V, i.e., the voltage for which the interband tunneling process starts. This potential profile is the basis for the calculation of the spin-current polarization within the transfer matrix formalism. An additional component of the potential profile used in the transfer matrix formalism is the bias ΔV that corresponds to the potential drop across the Zener diode when the bias on the whole spin-LED is changed. We assume a linear potential drop which fairly well renders the real band bending across the p–n junction.

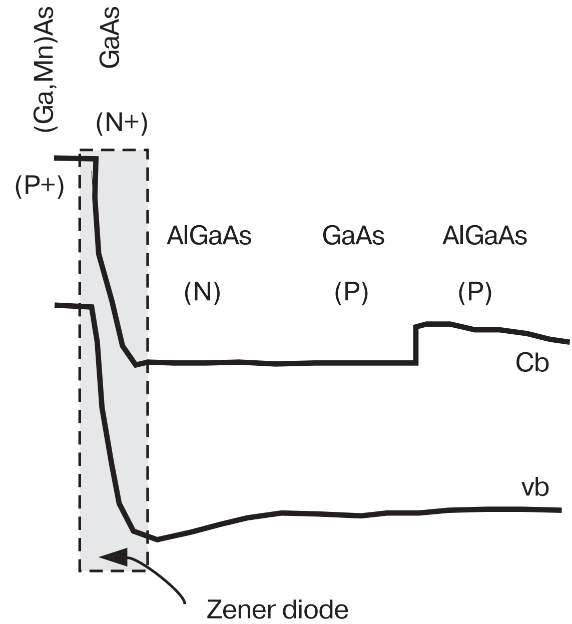

Fig. 1. Potential profile for the entire experimental structure at an external bias of V_0 = 1.81 V. In the calculations of the coherent current only the Zener diode region is considered.

In Fig. 2 the dependence of the current spin polarization on the external bias ΔV in the Zener tunneling diode is depicted. One can see that at low bias, the current spin polarization is of the order of 0.6, in good agreement with the experimental results (0.7–0.8). Interestingly, the current spin polarization decreases rapidly with ΔV. The strong dependence of current spin polarization on bias is again in agreement with the experimental findings, though a direct comparison is hampered by the fact that the exact relation between ΔV and the total bias V applied to the device is known only from simulations. Having these obstacles in mind and to reduce computational burden, the calculations for higher bias ($\Delta V > 0.1$ V) have been performed with lower accuracy. The latter is probably responsible for the spread of current spin polarizations obtained in this region.

It is pretty obvious that the degree of spin polarization of the tunnel current may depend on these intrinsic features of (Ga,Mn)As layers. For example, it is

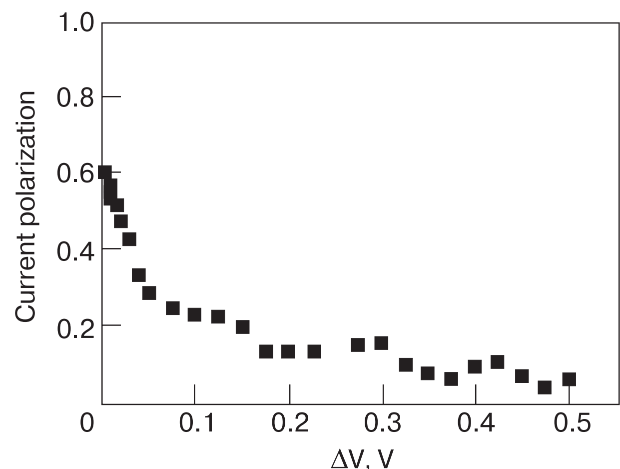

Fig. 2. The calculated current spin polarization as a function of external bias for the Zener diode.

well known that magnetic characteristics of (Ga,Mn)As depend strongly on both hole and manganese concentrations [8]. To investigate this problem, we have calculated the dependence of current spin polarization on the hole concentration p and Mn content x. For these calculations we assume that the electron concentration is $n = 10^{19}$ cm^{-3} as indicated by the experimental results in Ref. 12. The dependencies of the current spin polarization on the hole concentration p and Mn content $x = 0.08$ are depicted in Fig. 3. These results show a strong decrease of the tunneling current spin polarization with the increase of hole concentration. The spin injection in the Zener diode depends also crucially on the content of magnetic ions in the $Ga_{1-x}Mn_x$ layer. For $x = 0.08$, we obtain the spin current polarization of the order of 60%, which agrees fairly well with the observations in [12].

Another problem in studies of spin currents is the role of anisotropy, since (Ga,Mn)As layers exhibit a variety of anisotropic properties [8,29,30]. We have also studied anisotropy effects in spin polarization of the tunneling current in the Zener diode within developed the scattering formalism developed, gaining some insight into physical mechanism leading to such anisotropy [31].

3.2. Tunneling magnetoresistance

Now we demonstrate how the whole TMR semiconductor structures can be modeled by the formalism developed. In our calculations of the TMR effect we consider the structure consisting of three layers. The two half-infinite leads are build made of ferromagnetic p-type $Ga_{1-x}Mn_xAs$. The middle, scattering region is composed of the nonmagnetic GaAs, which forms a barrier for the holes. We compare the tunneling currents in two configurations, i.e., with parallel (ferromagnetic — FM) and the antiparallel (antiferromagnetic — AFM) alignments of the spontaneous magnetizations in the leads. We define the TMR as

$$\mathrm{TMR} = \frac{I_{FM} - I_{AFM}}{I_{AFM}}, \tag{8}$$

where I_{FM} and I_{AFM} are the currents in the FM and AFM configurations of the spontaneous magnetizations in the leads, respectively. In Fig. 4,*a* the TMR values obtained, for a given (8%) Mn content and a set of different hole concentrations in the FM layers are plotted as a function of the applied bias.

As can easily be seen from the Fig. 4, TMR depends strongly on the hole concentration. As TMR is determined primarily by the spin polarization of the carriers at the Fermi level, this is in agreement with the result of Ref. 8 stating that the higher the hole concentration the smaller is the polarization at the Fermi level. For $p = 3.5 \cdot 10^{20}$ cm^{-3}, which is the typical hole concentration in (Ga,Mn)As samples with high Mn content [32], a TMR of about 250% has been obtained.

Recent experiments show that in $Ga_{1-x}Mn_xAs$ samples the Fermi energy of the hole liquid remains equal about 220 meV for a wide range of Mn content and that the hole concentration depends very little on x [33] — thus, in the following we have calculated a TMR for different x in the magnetic layers, while the hole concentration in these regions is kept equal to $p = 3.5 \cdot 10^{20}$ cm^{-3}. The results of this study are presented in Fig. 4,*b*.

Surprisigly enough, our simple model fully reproduces the experimental data: for structures with 8% of

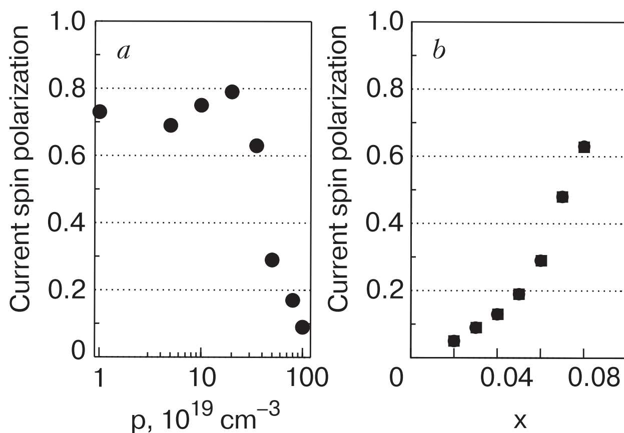

Fig. 3. Spin current polarization in p-$Ga_{1-x}Mn_xAs$/n-GaAs as a function of hole concentration p for $x = 0.08$ (*a*); Mn content x for $p = 3.5 \cdot 10^{20}$ cm^{-3} (*b*). The bias applied to the structure is $V = 0.05$ V.

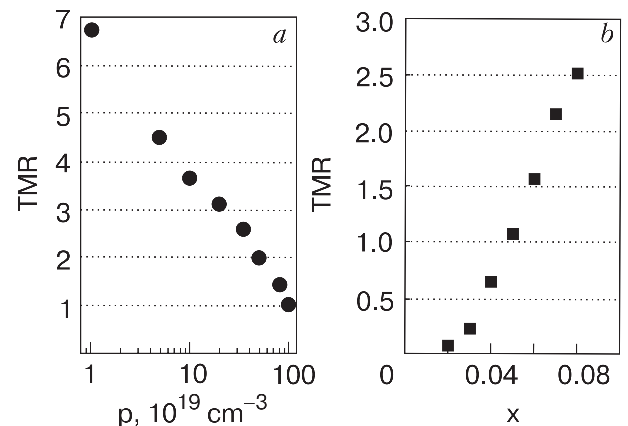

Fig. 4. TMR in $Ga_{1-x}Mn_xAs$/GaAs/$Ga_{1-x}Mn_xAs$ as a function of hole concentration p for fixed Mn content $x = 0.08$ (*a*); as a function of Mn content for fixed hole concentration $p = 3.5 \cdot 10^{20}$ cm^{-3} (*b*). The bias applied to the structure is $V = 0.05$ V.

Mn we obtain the TMR of the order of 250%, as observed recently by Chiba et al. [15]; for 4% Mn the calculations lead to a TMR of the order of 60%, in perfect agreement with the experimental observations [13,34]. Therefore, our calculations seem to suggest that for obtaining high TMR, large exchange splittings, i.e., high concentrations content of magnetic ions, are needed. Unfortunately, the presented in Fig. 4 dependence suggests that the attempts to increase the hole concentration in (Ga,Mn)As, in order to obtain higher Curie temperature, may result in much smaller TMR in the structure.

4. Summary

We have analyzed the vertical coherent spin transport in (Ga,Mn)As-based heterostructures using a tight-binding model together with the Landauer—Büttiker formalism. Our studies reproduce quantitatively the recently observed high TMR in (Ga,Mn)As/(Al,Ga)As/(Ga,Mn)As trilayers. Within the formalism we are able to study spin polarization of the current. The theoretical calculations of (Ga,Mn)As/(Al,Ga)As Zener diodes demonstrate large spin polarization of the injected current in excellent agreement with experimental results. The model reproduces as well the experimentally observed strong dependence of the spin polarization of the injected current and TMR effect on the applied bias voltage, both in Zener and TMR heterostructures. It should be pointed out that our calculations do not take into account, e.g., the interfacial roughness or the scattering on impurities or defects, magnons, and other physical effects that were previously ascribed to this intriguing bias dependence. Instead, the formalism employed describes carefully the electronic structure of the heterostructure, especially at the interfaces. In contrast to the standard $(k \cdot p)$-method, the scattering formalism based on the tight-binding scheme takes into account all the effects resulting from the electric field in the depletion zone, in particular Rashba and Dresselhaus terms which are essential for the lost of spin polarization. These features make the approach particularly suited for studying phenomena related to spin-polarized tunneling.

This work was partly supported by the EC project NANOSPIN (FP6-2002-IST-015728). Calculations were carried out using the resources and software at Interdisciplinary Center of Mathematical and Computer Modelling (ICM) in Warsaw.

1. For a review on III-V diluted magnetic semiconductors, see, F. Matsukura, H. Ohno, and T. Dietl, in: *Handbook of Magnetic Materials* **14**, K.H.J. Buschow (ed.), North-Holland, Amsterdam (2002).
2. H. Munekata, H. Ohno, S. von Molnar, Armin Segmüller, L.L. Chang, L. Esaki, and H. Ohno, *Phys. Rev. Lett*. **63**, 1849 (1989); H. Ohno, *Science* **281**, 951 (1998) and references therein.
3. M.N. Baibich, J.M. Broto, A. Fert, F. Nguyen Van Dau, F. Petroff, P. Eitenne, G. Creuzet, A. Friederich, and J. Chazelas, *Phys. Rev. Lett*. **61**, 2472 (1988).
4. G.A. Prinz, *Phys. Today* **48**, 58 (1995) and references therein.
5. D.J. Monsma, J.C. Lodder, Th.J.A. Popma, and B. Dieny, *Phys. Rev. Lett*. **74**, 5260 (1995).
6. Y. Ohno, D.K. Young, B. Beschoten, F. Matsukura, H. Ohno, and D.D. Awschalom, *Nature* **402**, 790 (1999).
7. H. Ohno, D. Chiba, F. Matsukura, T. Omiya, E. Abe, T. Dietl, Y. Ohno, and K. Ohtani, *Nature* **408**, 944 (2001).
8. T. Dietl, H. Ohno, and F. Matsukura, *Phys. Rev.* **B63**, 195205 (2001).
9. K.W. Edmonds, K.Y. Wang, R.P. Campion, A.C. Neumann, C.T. Foxon, B.L. Gallagher, and P.C. Main, *Appl. Phys. Lett*. **81**, 3010 (2002).
10. S. Datta and B. Das, *Appl. Phys. Lett.* **56**, 665 (1990).
11. M. Júlliere, *Phys. Lett*. **54A**, 225 (1975).
12. P. Van Dorpe, Z. Liu, W. Van Roy, V.F. Motsnyi, M. Sawicki, G. Borghs, and J. De Boeck, *Appl. Phys. Lett*. **84**, 3495 (2004).
13. M. Tanaka and Y. Higo, *Phys. Rev. Lett*. **87**, 026602 (2001).
14. R. Mattana, J.-M. George, H. Jaffrés, F. Nguyen Van Dau, A. Fert, B. Lépine, A. Guivarc'h, and G. Jézéquel, *Phys. Rev. Lett*. **90**, 166601 (2003).
15. D. Chiba, F. Matsukura, and H. Ohno, *Physica* **E21**, 966 (2004).
16. M. Elsen, O. Boulle, J.-M. George, H. Jaffrés, R. Mattana, V. Cros, A. Fert, A. Lemaître, R. Giraud, and G. Faini, *Phys. Rev*. **B73**, 035303 (2006).
17. A.G. Petukhov, A.N. Chantis, and D.O. Demchenko, *Phys. Rev. Lett*. **89**, 107205 (2002).
18. L. Brey, *Appl. Phys. Lett*. **85**, 1996 (2004).
19. P. Van Dorpe, W. Van Roy, J. De Boeck, G. Borghs, P. Sankowski, P. Kacman, J. A. Majewski, and T. Dietl, *Phys. Rev.* **B72**, 205322 (2005).
20. P. Sankowski, P. Kacman, J.A. Majewski, and T. Dietl, *Physica* **E32**, 375 (2006).
21. R. Oszwałdowski, J.A. Majewski, and T. Dietl, *Phys. Rev*. **B74**, 153310 (2006).
22. J.-M. Jancu, R. Scholz, F. Beltram, and F. Bassani, *Phys. Rev.* **B57**, 6493 (1998).
23. J. Okabayashi, A. Kimura, O. Rader, T. Mizokawa, A. Fujimori, T. Hayashi, and M. Tanaka, *Physica* **E10**, 192 (2001).
24. Aldo Di Carlo, P. Vogl, and W. Pötz, *Phys. Rev.* **B50**, 8358 (1994).

25. C. Strahberger and P. Vogl, *Phys. Rev.* **B62**, 7289 (2000).
26. Aldo di Carlo, *Semicond. Sci. Technol.* **18**, R1 (2003).
27. L. Brey, J. Fernandez-Rossier, and C. Tejedor, *Phys. Rev*. **B70**, 235334 (2004).
28. M. Kohda, T. Kita, Y. Ohno, F. Matsukura, and H. Ohno, *Appl. Phys. Lett.* **89**, 012103 (2006).
29. M. Sawicki, F. Matsukura, A. Idziaszek, T. Dietl, G. M. Schott, C. Ruester, C. Gould, G. Karczewski, G. Schmidt, and L.W. Molenkamp, *Phys. Rev.* **B70**, 245325 (2004).
30. M. Sawicki, K.-Y. Wang, K.W. Edmonds, R.P. Campion, C.R. Staddon, N.R.S. Farley, C.T. Foxon, E. Papis, E. Kaminska, A. Piotrowska, T. Dietl, and B.L. Gallagher, *Phys. Rev.* **B71**, 121302(R) (2005).
31. P. Sankowski, P. Kacman, J.A. Majewski, and T. Dietl, *Phys. Rev.* **B75**, 045306 (2007).
32. K.M. Yu, W. Walukiewicz, T. Wojtowicz, W.L. Lim, X. Liu, Y. Sasaki, M. Dobrowolska, and J.K. Furdyna, *Appl. Phys. Lett.* **81**, 844 (2002).
33. V. Osinniy, K. Dybko, A. Jedrzejczak, M. Arciszewska, W. Dobrowolski, T. Story, M.V. Radchenko, V.I. Sichkovskiy, G.V. Lashkarev, S.M. Olsthoorn, and J. Sadowski, *http://arXiv.org/cond-mat/0409659*.
34. J.-M. George, H. Jaffres, R. Mattana, M. Elsen, F. NGuyen Van Dau, A. Fert, B. Lepine, A. Guivarc'h, and G. Jezequel, *Molecular Phys. Rep.* **40**, 23 (2004).